Research Article

Inas Al-Qadsy, Waseem Sharaf Saeed*, Abdel-Basit Al-Odayni, Ali Alrabie, Lena Ahmed Saleh Al-Faqeeh, Arwa Al-Adhreai, Ahmad Abdulaziz Al-Owais, Abdelhabib Semlali, Mazahar Farooqui*

Antidiabetic, antioxidant and cytotoxicity activities of *ortho*- and *para*-substituted Schiff bases derived from metformin hydrochloride: Validation by molecular docking and *in silico* ADME studies

https://doi.org/10.1515/chem-2023-0125
received August 6, 2023; accepted August 31, 2023

Abstract: This work evaluates the *in vitro* antioxidant and antidiabetic activities of two metformin hydrochloride-based Schiff bases. Moreover, the 3-(4,5-dimethylthiazol-2-yl)-2,5-diphenyl tetrazolium bromide (MTT) assay was used to examine the *in vitro* cytotoxic effects of HL1 and HL2 on the A549 lung cancer cell line. The two Schiff bases that have been previously synthesized by using two effective, green techniques, namely stirring and microwave-assisted, are *N*,*N*-dimethyl-*N*′-[(*Z*)-(2-nitrophenyl) methylidene] imidodicarbonimidic diamide and *N*,*N*-dimethyl-*N*′-[(*Z*)-(4-nitrophenyl) methylidene] imidodicarbonimidic diamide, indicated by HL1 and HL2, respectively. Studies of antidiabetic efficacy using alpha-amylase revealed that HL2 has a higher inhibition than HL1, but the results on sucrase enzyme showed that HL1 had the highest inhibitory action, whereas the outcome of the antioxidant test with the 2,2-diphenyl-1-picrylhydrazyl assay demonstrated that HL2 was the most effective antioxidant, followed by ascorbic acid and HL1. In the MTT assay, HL1 had the best result, with an IC_{50} value of 57.13 µg/mL compared to HL2 with an IC_{50} value of 76.83 µg/mL. It was observed that HL1 was the most effective against the human lung cancer cell line A459. The findings were supported by computational and pharmacokinetic studies (SwissADME). Based on empirical and computational studies, we suggest that HL1 and HL2 are promising candidates as antioxidants and antidiabetics after being examined *in vivo*.

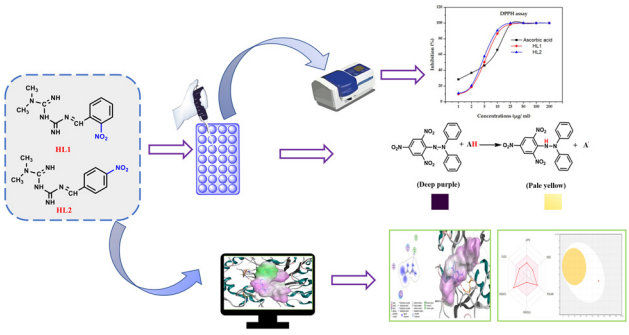

Graphical abstract

Keywords: Schiff bases of metformin hydrochloride, 2,2-diphenyl-1-picrylhydrazyl (DPPH) radical, alpha-amylase, sucrase enzymes, antidiabetic, cytotoxicity assay, docking study, swissADME properties

*** Corresponding author: Waseem Sharaf Saeed**, Department of Restorative Dental Sciences, College of Dentistry, King Saud University, P.O. Box 60169, Riyadh 11545, Saudi Arabia, e-mail: wsaeed@ksu.edu.sa
*** Corresponding author: Mazahar Farooqui**, Chemistry Department, Maulana Azad College of Arts, Science and Commerce, Aurangabad 431001, India, e-mail: mazaharf@maca.ac.in
Inas Al-Qadsy, **Ali Alrabie**, **Arwa Al-Adhreai:** Chemistry Department, Maulana Azad College of Arts, Science and Commerce, Aurangabad 431001, India
Abdel-Basit Al-Odayni: Department of Restorative Dental Sciences, College of Dentistry, King Saud University, P.O. Box 60169, Riyadh 11545, Saudi Arabia
Lena Ahmed Saleh Al-Faqeeh: Microbiology Department, Dr. Babasaheb Ambedkar Marathwada University, Aurangabad 431004, India
Ahmad Abdulaziz Al-Owais: Chemistry Department, College of Science, King Saud University, P.O. Box 2455, Riyadh 11451, Saudi Arabia
Abdelhabib Semlali: Groupe de Recherche en Écologie Buccale, Faculté de Médecin Dentaire, Université Laval, Quebec, QC G1V 0A6, Canada

1 Introduction

Important organic compounds known as “Schiff bases” have a carbon–nitrogen double bond, with the nitrogen

atom attached to either an aryl or an alkyl group. They form when an amine condenses with a carbonyl substance, generally an aldehyde or a ketone.

They have a variety of biological effects, such as antidiabetic, antioxidant, and antitumor abilities, and they are desirable candidates for drug development and additional pharmacological and medicinal chemistry research due to their adaptability and prospective therapeutic applications [1–5].

Hyperglycemia is caused by abnormalities in insulin secretion, action, or both that characterize diabetes mellitus (DM). According to the World Health Organization, there are two types of DM: type (I) insulin-dependent diabetes mellitus and type (II) noninsulin-dependent diabetes mellitus (NIDDM). A complete lack of insulin secretion is the root cause of type (I), while a combination of insulin resistance and an insufficient compensatory insulin-secretory response causes type (II) diabetes [6–8]. Diabetes affects 371 million people worldwide, with 90% of people developing type (II) diabetes as a result of their lifestyle, genetic tampering in (agriculture and dietary products) and a lack of physical exercise. The most prominent symptoms are increased thirst, hunger, polyuria, blurred vision, and weight loss. Over time, DM can lead to cardiovascular disease (five million people died in 2011), sexual dysfunction, neuropathy, nephropathy (which can lead to renal failure), cancer, and stroke [9–14].

Type (I) diabetes requires insulin injections to compensate for lack of insulin production and affects the remaining 10% of people, whereas type (II) diabetes is treated with oral medications such as biguanides, sulfonylureas, tolbutamide, glinides, α-glucosidase inhibitors, thiazolidinediones, phenformin, troglitazone, repaglinide, and rosiglitazone [9,13,15,16].

Researchers are focusing on developing diabetes treatments such as lifestyle changes, diet modifications, weight management, regular exercise, herbal therapy, and traditional drugs (oral and injectable) to delay carbohydrate absorption [9,17–24].

Even though metformin is the most extensively used oral antidiabetic medication and has significant advantages over other treatments, 20–30% of the patients experience gastrointestinal side effects, and 5% cannot tolerate it. Metformin, which is derived from the medicinally named plant *Galega officinalis* and was historically used to treat diabetes in medieval Europe, is still the only ethical medicine licensed for the treatment of NIDDM patients [22,25,26].

Furthermore, the emergence of diabetes problems has been linked to oxidative stress and free radical overproduction. Atom or molecule fragments with one or more unpaired electrons in atomic or molecular orbitals are called free radicals, which are often unstable, so they assault the nearest stable molecule as soon as possible to collect the electron that it requires to gain stability [27]. The two types of free radicals that are most frequently produced in the human body are reactive oxygen species (ROS) and reactive nitrogen species. Both endogenous and exogenous sources produce free radicals, exogenous sources such as pollution, alcohol, tobacco smoke, heavy metals, transition metals, industrial solvents, pesticides, certain drugs like halothane, paracetamol, and radiation, as well as endogenous sources such as mitochondria, peroxisomes, endoplasmic reticulum, phagocytic cells, and so on [28–32].

Oxidative stress is caused by high concentrations of reactive free radical species, which can damage nucleic acids, lipids, proteins, and cell structure. It can also lead to many diseases, such as lung disease, liver disease, cirrhosis, heart disease, atherosclerosis, diabetes, rheumatoid arthritis, and Parkinson's disease. So, free radical production and antioxidant defenses need to be in balance for an organism to function properly [29–37].

Antioxidants are substances found in small amounts in the body compared to free radicals. Enzymatic and nonenzymatic antioxidants are two types of antioxidants that scavenge unpaired electrons, prevent the generation of free radicals, stop chain reactions, and dampen the energy of executed molecules [27,31].

Natural and synthetic antioxidants are two types of antioxidants that stabilize free radicals and suppress them. Natural antioxidants are composed of minerals, vitamins, and phytochemicals. Minerals are essential for enzymatic processes, and vitamins are essential for redox reaction regulation. Phytochemicals suppress free radical reactivity by stabilizing free radicals. Synthetic antioxidants are phenolic compounds that interact with free radicals to suppress free radical chain reactions. Plant and fungi extracts contain antioxidant compounds such as flavones, isoflavones, flavonoids, anthocyanins, coumarins, lignans, catechins, and isocatechins [27,31,38].

It is also fascinating to note that metformin has been linked to a variety of biological processes, including weight loss, anti-aging, and anticancer action [39,40].

Since 10 years ago, increasing evidence has emerged suggesting that biguanide medications like metformin may be helpful in the prevention and treatment of a variety of cancers, such as prostate cancer [41]. Individuals with DM in particular have a higher chance of developing cancer, and metformin has been discovered to significantly inhibit a number of malignancies [42,43].

Previously, two novel Schiff bases HL**1** and HL**2**, were successfully synthesized via an eco-friendly methodology and characterized using elemental analysis, differential scanning calorimetry, fourier-transform infrared spectroscopy, UV–Vis spectroscopy, ^{1}H NMR spectroscopy, ^{13}C NMR spectroscopy, and mass spectroscopy. The antibacterial

activity of both metformin derivatives was evaluated using the agar well diffusion method against a range of gram-positive and gram-negative pathogens [6].

Our current work focuses on evaluating the *in vitro* cytotoxic, antidiabetic, and antioxidant tests of metformin derivatives (HL1 and HL2). The inhibition of α-amylase and sucrase enzymes by Schiff bases HL1 and HL2 was used to measure the level of antidiabetic activity. In contrast, the 2,2-diphenyl-1-picrylhydrazyl (DPPH) test was used to measure the antioxidant activity of metformin derivatives while assessing their cytotoxic effects on the A549 lung cancer cell line using the 3-(4,5-dimethylthiazol-2-yl)-2,5-diphenyl tetrazolium bromide (MTT) test. Molecular docking studies were carried out to investigate the possible binding mechanisms of HL1 and HL2 with their target proteins in order to support their antioxidant and antidiabetic effects. Additionally, absorption, distribution, metabolism, and excretion (ADME) is used for predicting the medicinal chemistry and drug-like characteristics of metformin derivatives.

2 Materials and methods

2.1 Synthesis of metformin Schiff bases HL1 and HL2

Earlier, our study was done on the synthesis of the metformin-based Schiff bases HL1 and HL2, utilizing both conventional and green techniques. In the traditional procedure, equimolar quantities of metformin-HCl and (*ortho*) *para*-substituted benzaldehyde were refluxed in methanolic basic medium. In the environmentally friendly procedures, equimolar solutions of metformin and nitro-substituted benzaldehydes were dissolved in a basic aqueous medium and either refluxed under microwave irradiation (Method I) or stirred at room temperature using a magnetic stirrer (Method II) [6].

2.2 Biological tests

2.2.1 Antioxidant

The antioxidant efficacy of HL**1** and HL**2** was measured using the DPPH test.

2.2.1.1 Procedure

In vitro, antioxidant efficiency was assessed by the DPPH assay with few adjustments [32]. About 0.05 mL of HL**1** and HL**2** dissolved in methanol were diluted to 1.0 mL using ethanol to attain concentrations of 1–200 µg/mL and were added with DPPH (final concentration: 200 µM, in 95% ethanol). The control contains dimethyl sulfoxide (DMSO) and ethanol in similar amounts. Triplicate aliquots were used for each test. The reference standard (positive control) applied was ascorbic acid. A decrease in the absorbance of the test compounds was detected at 515 nm after 20 min using UV–vis spectroscopy (Shimadzu UV-1800, Tokyo, Japan), and the following formula was used for calculating the % inhibition:

$$\% \text{ Scavenging activity} = \frac{(\text{Control absorbance} - \text{Sample absorbance})}{(\text{Control absorbance})} \times 100.$$

The sample absorbance is the measurement of the DPPH solution with compounds, whereas the control absorbance is the measurement of the DPPH solution without compounds.

2.2.2 Antidiabetic

In vitro, the antidiabetic activity of HL**1** and HL**2** was estimated by how well they blocked the actions of the enzymes alpha-amylase and sucrase.

2.2.2.1 Procedure for the alpha-amylase inhibition assay

The alpha-amylase inhibition assay was carried out according to the protocol outlined by Puneeth and Sharada [44]. The alpha-amylase enzyme (1 unit/mL) from *Bacillus* species was dissolved using 0.1 M phosphate-buffered saline (pH 6.9). The enzyme solution was pre-incubated with the various concentrations of HL1 and HL2 (50, 100, and 200 µg) for 10 min at 37°C. The enzymatic reaction was allowed to occur for 30 min at 37°C after the starch solution (0.1%) was added to the incubation medium to start the reaction. By adding 3,5-dinitrosalicylic acid (DNS reagent) to the reaction mixture, the reaction was stopped. The tubes were then placed in a boiling water bath for 10 min. By adding a 40% sodium potassium tartrate solution and allowing it to cool to room temperature, the color was stabilized. At 540 nm, the optical density was determined. A positive control was used, which was metformin. The following formula was used to determine the compounds' % activity:

$$\% \text{ Activity} = \frac{\text{Sample absorption}}{\text{Control absorption}} \times 100.$$

2.2.2.2 Procedure for the sucrase inhibition assay

The inhibitory studies of HL**1** and HL**2** on sucrase enzyme were performed based on the procedure given by Sharath

Chandra et al. [45] with a few changes. In brief, HL1 and HL2 were pre-incubated with enzyme solution at various concentrations (50, 100, and 200 µM) in maleate buffer (0.1 M, pH 6) for 10 min at 37°C. Sucrose solution (60 mM) was added to start the reaction and incubated for 30 min at 37°C. After incubation, the reaction was stopped by placing the reaction mixture in a water bath for 10 min. The amount of glucose liberated in the reaction mixture was estimated using the glucose oxidase–peroxidase method (GOD–POD strategy).

2.2.2.3 Estimation of glucose by the GOD–POD method

The glucose generated in the mixture of reaction was calculated by the GOD–POD test kit instructions [45]. In short, 50 µL of the incubated medium was added to a 96-well ELISA plate. Each well received 200 µL of the GOD-POD color reagent and then will be incubated for 30 min at 37°C in the dark for the development of color. At 505 nm the optical density was determined. Metformin was used as a positive control. The following formula was used to calculate each compound's % activity:

$$\% \text{ Activity} = \frac{\text{Sample absorption}}{\text{Control absorption}} \times 100.$$

2.2.3 Cytotoxicity assay

Ligands HL**1** and HL**2** were examined for *in vitro* cytotoxicity against the A549 lung cancer cell line obtained from the DSMZ Leibniz Institute (German Collection of Microorganisms and Cell Cultures Braunschweig, Germany). The cell viability assay was performed by the MTT method, which was provided by Invitrogen, Waltham, MA, USA. The solvent used for preparation (DMSO, acidified isopropanol) obtained from Sigma, St. Louis, MO, USA, UV–vis analysis Nuaire, Plymouth, MN, USA.

The 3-(4,5-dimethylthiazol-2-yl)-2,5-diphenyl tetrazolium bromide (MTT) test was used to measure cell viability as already mentioned [46–48].

The cytotoxic activity of the synthesized compounds (HL**1** and HL**2**) was evaluated *in vitro* using the MTT assay. In brief, the A549 lung cancer cell line was grown for 24 h at 37°C after being plated at a density of 5×10^4 cells per well in a 24-well plate. Following that, the cells were subjected to various concentrations (100, 50, 25, and 12.5 µg/mL) of each substance. About 100 µL of MTT (5 mg/mL in phosphate-buffered saline) was added to each well after 48 h of incubation. After a further 4 h at 37°C incubation of the plates, the formazan crystals were dissolved in 1 mL of acidified isopropanol. The cell viability was calculated at 570 nm using the following formula:

$$\% \text{ Cell viability} = \frac{\text{Mean absorbance of treated cells}}{\text{Mean absorbance control}} \times 100$$

The dose–response curve was used to get the inhibitory concentration (IC_{50}) value.

2.2.4 Statistical analysis

Mean ± standard error is used to display experimental data. Statistical analyses were carried out by one-way ANOVA using SPSS ver. 20.0 software.

2.3 Software program

2.3.1 Molecular docking using molecular operating environment (MOE)

By using a protein data bank (http://www.rcsb.org/pdb, accessed on 30 August 2022), the X-ray crystal structures of water-forming NAD (P) H oxidase (PDB ID: 2CDU, 1.80 Å resolution) and human pancreatic α-amylase (PDB ID: 1B2Y with a resolution of 3.20 Å) were retrieved [49,50]. For docking, the MOE was utilized for preparing the protein structures. First, the Sequence Editor window of MOE was used to remove undesirable atoms, molecules, chains, and ligands (**2CDU**: H_2O molecules, co-crystallized ligands ADP and FAD were removed [51]; **1B2Y:** H_2O molecules, ion metals, and the PCA ligand were removed). Second, polar hydrogen atoms were added. Third, energy was minimized using Amber12.EHT with an RMS of 0.1 kcal/mol/A^2. Fourth, missing atoms were corrected and typed (2CDU: 6,943 atoms; 1B2Y: 7,763 atoms). Fifth, the site finder module of MOE was utilized to identify protein's active site (2CDU: the largest pocket contains 229 amino acids, IB2Y: the ligand pocket contains 129 amino acids). ChemDraw was used to draw the ligands' 2D structures, while MOE software (protonation, partial charges, and energy minimization) was utilized to prepare 3D structures. At last, the database file of ligands was created and saved for further docking [52,53].

In order to locate and analyze the interaction between ligand and protein, docking was conducted with certain settings (Rescoring function1 and rescoring function 2: London dG, placement: Triangle matcher, retain:2 and Refinement: force field). After that, the compound that had the best overall characteristics in terms of energy, H-bond count, and location was selected as the one to be visualized [54,55].

2.3.2 SwissADME

SwissADME is a free web application on a website (http://www.swissadme.ch/, accessed on 20 July 2022). ADME supports the development of new drugs by precisely predicting the medicinal chemistry, drug-like properties, solubility, lipophilicity (LIPO), physicochemical properties, and pharmacokinetic parameters of small molecules [56].

SwissADME also exhibited the structure and bioavailability radar using canonical SMILES. The first part showed the chemical structure in two dimensions. The second part is the bioavailability radar, which allows for a rapid peek at how much the target compounds resemble medicines. For each feature anticipated to be orally accessible, the optimum physicochemical environment is illustrated by the pink area as LIPO: −0.7 < XLOGP3 < +5.0, SIZE (Molecular weight (MW)) 150 g/mol < MW < 500 g/mol, POLAR (Polarity) 20Å^2 < Molecular polar surface area (TPSA) < 130 Å^2, INSOLU (Insolubility) −6 < Log S(ESOL) < 0, INSATU (Insaturation) 0.25 < FractionCsp3 < 1 and FLEX (Flexibility) 0 < RP (Number of rotatable bonds) < 9 are the six physicochemical qualities that are taken into consideration [57].

3 Results and discussion

HL**1** and HL**2** in Scheme 1 represent the Schiff bases derived from metformin hydrochloride and substituted (*ortho*)*para*-nitrobenzaldehyde, and they have been effectively synthesized utilizing conventional and microwave-assisted techniques earlier published [6].

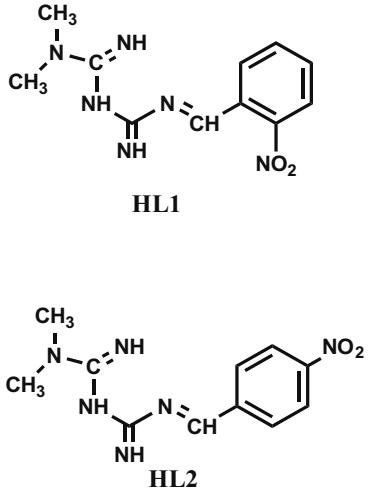

Scheme 1: Chemical structures of Schiff bases HL**1** and HL**2.**

The DPPH test was used to examine the antioxidant activity of HL**1** and HL**2**. Besides that, the alpha-amylase and sucrase enzymes were inhibited to assess the antidiabetic activity of metformin derivatives, and the result is supported by a docking study and SwissADME prediction.

3.1 *In vitro* study

3.1.1 Antioxidant

The scavenging activity of the free radical DPPH was investigated with minor modifications [58] by the spectrophotometric method.

The scavenging mechanism of free radical DPPH is the reduction process, as depicted in Figure 1. The stable free radical DPPH has the color purple, but when either HL**1** or HL**2** is added, DPPH gets a proton and turns yellow [59].

Table 1 and Figure 2 include the results of HL1 and HL2's antioxidant activity. Both exhibited significant antioxidant activity. HL**2** had the strongest antioxidant action and then ascorbic acid and HL**1,** with IC_{50} values of 4.89, 5.24, and 5.35 µg/mL, respectively.

3.1.2 Antidiabetic

3.1.2.1 Alpha-amylase inhibition activity

The alpha-amylase inhibitory activity results and IC_{50} are presented in Figure 3 and Table 2 for HL**1**, HL**2,** and standard metformin. HL**1** and HL**2** inhibited α-amylase most effectively when compared to regular metformin. HL**2** has the greatest level of inhibitory activity with an IC_{50} of 76.1 µg/mL, followed by HL**1** with an IC_{50} of 99.3 µg/mL. Metformin had very little potency against α-amylase with an IC_{50} of 272.6 µg/mL.

3.1.2.2 Sucrase inhibition activity

Table 3 and Figure 4 show that both HL1 and HL2 and standard metformin can stop sucrase enzymes from working. According to the observations, HL**1** showed the maximum inhibition activity with an IC_{50} of 89.3 µg/mL, followed by HL**2** and metformin with an IC_{50} of 93.3 and 492.4 µg/mL, respectively. Standard metformin displayed a relatively low level of sucrase enzyme inhibitory action.

3.1.3 MTT assay

Through the use of the MTT assay, cytotoxicity was identified. This assay based on the reduction of the

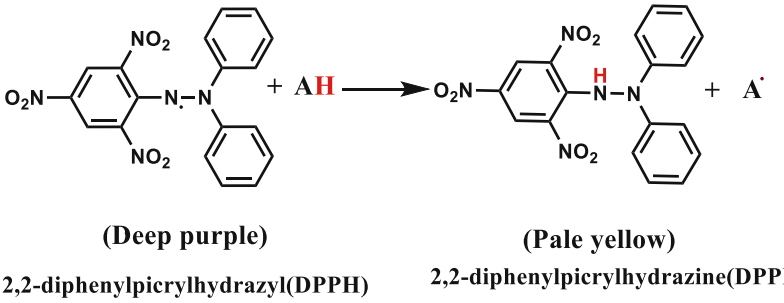

Figure 1: Mechanism of reduction DPPH to DPPHH using HL**1** and HL**2**(AH).

Table 1: Antioxidant activity of HL**1**, HL**2** and ascorbic acid

Compounds and standard	IC_{50} (μg/mL) ± standard error
HL**1**	5.35 ± 0.23
HL**2**	4.89 ± 0.34
Ascorbic acid	5.24 ± 1.38

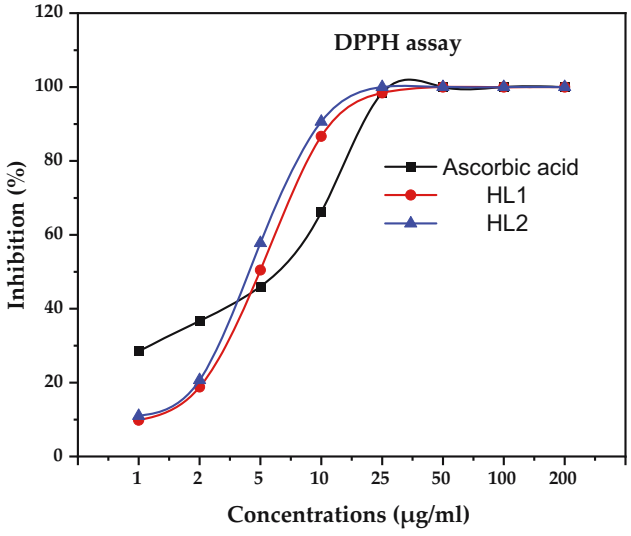

Figure 2: Scavenging activity (DPPH assay) of HL1, HL2, and ascorbic acid.

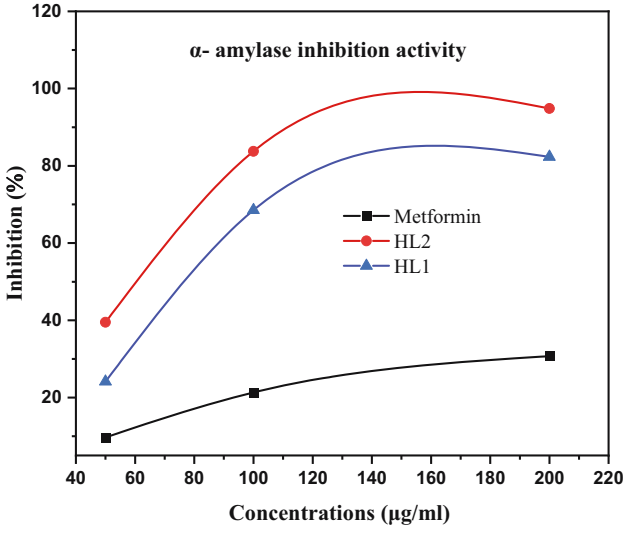

Figure 3: Percentage of inhibition activity of HL**1**, HL**2**, and metformin on α-amylase enzyme.

Table 2: IC_{50} of HL**1**, HL**2** and standard metformin

Compounds and standard	IC_{50} (μg/mL) ± standard error
HL**1**	99.3 ± 14.1
HL**2**	76.1 ± 14.6
Metformin	272.6 ± 27.2

Table 3: IC_{50} of HL**1**, HL**2**, and standard metformin

Compounds and standard	IC_{50} (μg/mL) ± standard error
HL**1**	89.3 ± 15.5
HL**2**	93.3 ± 14.7
Metformin	492.4 ± 16.4

calorimetrically measurable yellow tetrazolium salt 3-[4,5-dimethylthiazol-2-yl]-2,5-diphenyl tetrazolium bromide (MTT) into the purple formazan. This mechanism occurs in the mitochondria of metabolically active cells and indirectly measures cellular metabolic activity.

The cytotoxicity activity of HL**1** and HL**2** against the A549 lung cancer cell line is represented in Table 4 and Figure 5. To assess the cytotoxicity of Schiff bases, the lung cancer cell line A549 has been used. The MTT assay was performed to check each compound's cytotoxicity after 48 h of treatment with various concentrations. Results obtained indicated that at concentrations of 12.5, 25, 50, and 100 μg/mL, HL**1** showed inhibition activity against the A549 lung cancer cell line at 93.42, 68.24, 56.23, and 13.49%, respectively. IC_{50} of HL**1** was 57.13 μg/mL, but HL**2** has inhibition activities of 87.59, 76.19, 65.47, and 37.38%,

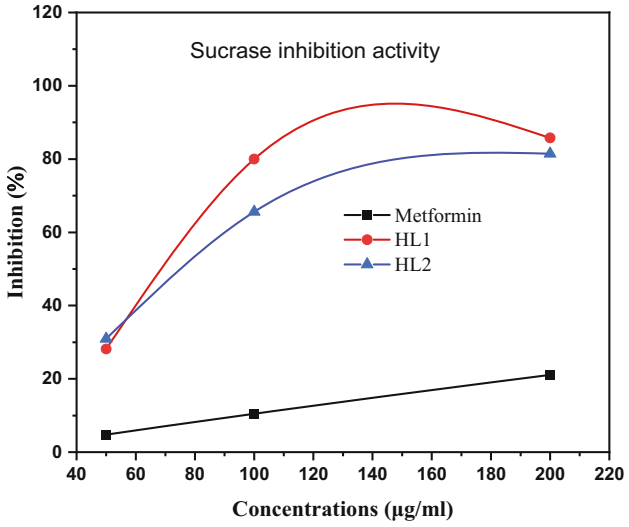

Figure 4: Percentage of inhibition activity of HL**1**, HL**2**, and metformin on sucrase enzyme.

Table 4: IC_{50} of HL**1** and HL**2** on A549 lung cancer cell line

Compounds	A549 IC_{50} (µg/mL)
HL**1**	57.13 ± 1.3
HL**2**	76.83 ± 2.3

Note: All IC_{50} values are described as mean ± SEM (n = 3).

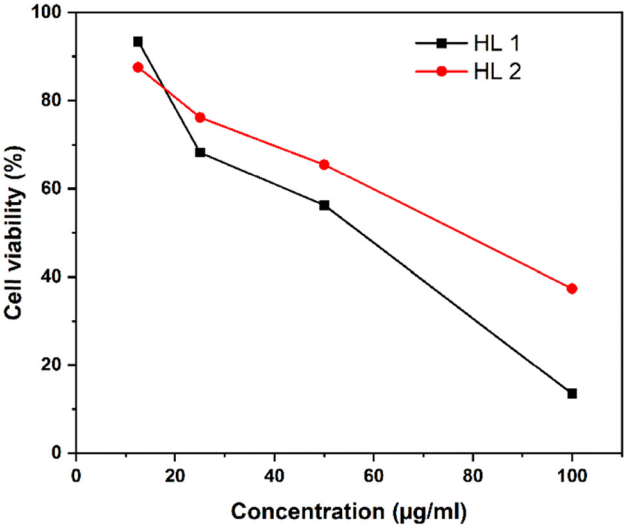

Figure 5: Cytotoxic activity of HL1 and HL2 against A549 lung cancer cell line.

respectively. Actually, compound HL**2** demonstrated a less potent cytotoxic effect on cell line A549 lung cancer (IC_{50} = 76.83) [60,61].

3.2 Theoretical study

3.2.1 Docking study

Molecular docking studies are routinely utilized in the pharmaceutical industry to assess the efficacy of new drug candidates. The binding mode in which bioactive compounds (also known as ligands) interact with their target proteins provides a useful way to categorize these compounds.

3.2.1.1 Antioxidant

The findings of our experiments indicate that our compounds have a significant potential for exhibiting antioxidant activity. To corroborate these findings, we carried out a molecular docking analysis to gain a deeper comprehension of one of the potential mechanisms underlying these findings. Then, due to its essential function in the production of ROS, we chose the NADPH enzyme (PDB code: 2CDU). According to the research that has been done, this enzyme is a significant contributor to the production of superoxide anion (O_2^-), which is the precursor to the vast majority of other ROS. Because of this, chemicals that are capable of inhibiting the NADPH oxidase (NOX) contribute significantly to the overall equilibrium of oxidative stress. The result indicates that HL**2** was the highest effective antioxidant. With a docking score of −6.49 kcal/mol, it outperformed both ascorbic acid (−5.04 kcal/mol) and HL**1** (−4.9 kcal/mol), as shown in Table 5 and Figures 6–8. At the protein's active site, it made two hydrogen bonds with amino acid residues ASP282 and CSX42 at distances of 2.94 and 4.23 Å, respectively (Figure 7). Furthermore, it formed two ionic interactions with ASP282 at 3.33 and 2.94 Å, respectively. HL**1** formed one hydrogen bond with the amino acid residue ASP282 at a distance of 3.30 and two ionic bond contacts with ASP282 at distances of 3.46 and

Table 5: Docking results of HL**1**, HL**2**, and ascorbic acid with 2CDU

Ligand	Ligand–protein interactions	Type of bond/ bond length (Å)	Docking score (kcal/mol)
HL**1**	Lig-NH-H—O-ASP282	H-donor/3.30	−4.9
	Lig—ASP282	Ionic/3.46	
	Lig—ASP282	Ionic/3.30	
HL**2**	Lig-NH-H—O-ASP282	H-donor/2.94	−6.49
	Lig-NH-H—S-CSX42	H-donor/4.23	
	Lig—ASP282	Ionic/3.33	
	Lig—ASP282	Ionic/2.94	
Ascorbic acid	Lig-O-H—O-SER41	H-donor/2.98	−5.04
	Lig-O-H—O-THR112	H-donor/3.07	
	Lig-O—H-ASP282	H-acceptor/3.20	

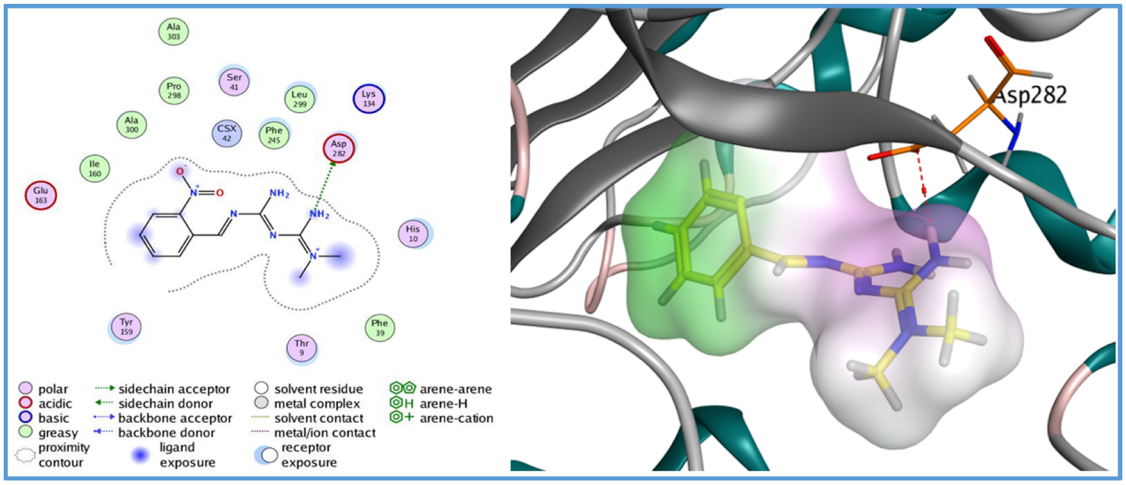

Figure 6: 2D and 3D of HL**1** at the active site of NAD (P) H oxidase (PDB ID: 2CDU).

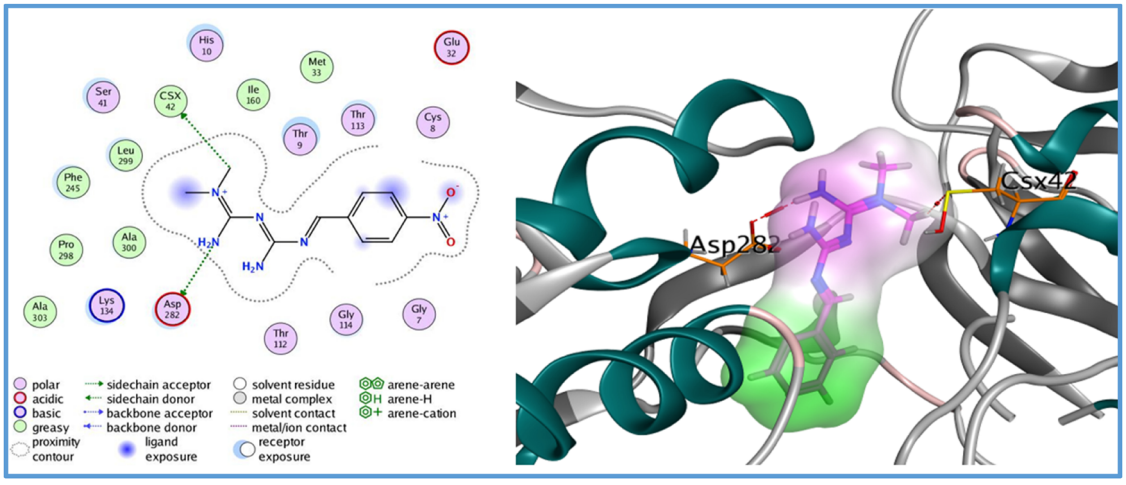

Figure 7: 2D and 3D of HL**2** at the active site of NAD (P) H oxidase (PDB ID: 2CDU).

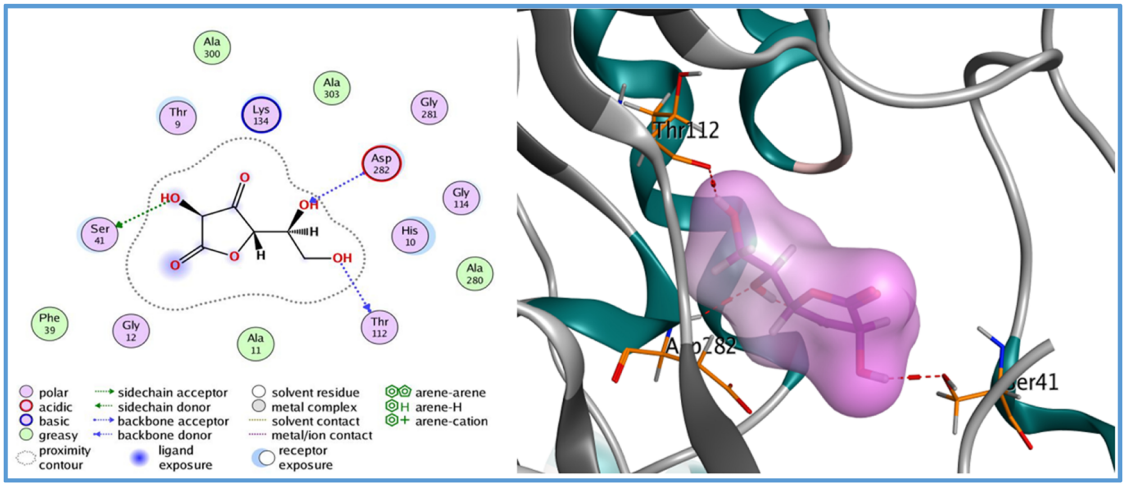

Figure 8: 2D and 3D of ascorbic acid at the active site of NAD (P) H oxidase (PDB ID: 2CDU).

3.30 Å. However, it does not interact with the important amino acid CSX42, as shown in Figure 6.

3.2.1.2 Antidiabetic activity

The examined compounds demonstrated a more significant association between *in vitro* activity and *in silico* study results, according to the docking results of these compounds against human pancreatic alpha-amylase (PDB ID: 1B2Y). The findings of the docking analysis showed that the metformin derivatives (Hl**1** and HL**2**) have higher negative docking scores (−5.41 and −5.47 kcal/mol) than metformin (−4.95 kcal/mol), which suggests that these two derivatives have strong affinities and excellent interactions (hydrogen bonds) within the active binding site of 1B2Y.

Three hydrogen bond interactions (red dashes) were formed between HL**1** and amino acid residues SER145, ASN105, and ASP147 at distances of 3.17, 3.36, and 2.85 Å respectively, as shown in the 2D and 3D representations of HL**1** in Figure 9. It also interacted with the amino acid residue ASP147 via an ionic interaction at a distance of 3.34 Å. HL2, on the other hand, formed two hydrogen bonds and two ionic interactions (Figure 10, Table 6). It formed two hydrogen bond interactions with amino acid residues SER145 and ASN105 at distances of 3.33 and 3.05 Å, respectively, and two ionic bond interactions with amino acid residue ASP147 at distances of 3.33 and 3.90 Å. The standard drug (metformin) formed only one hydrogen bond with amino acid LEU162 at a distance of 3.28 Å as shown in Figure 11.

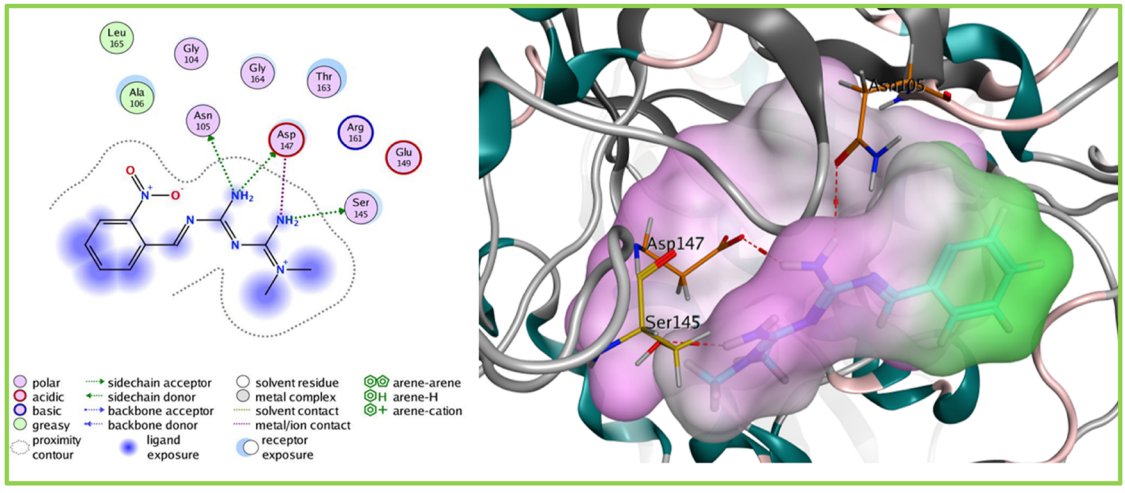

Figure 9: 2D and 3D of HL**1** at the active site of α-amylase (PDB: 1B2Y).

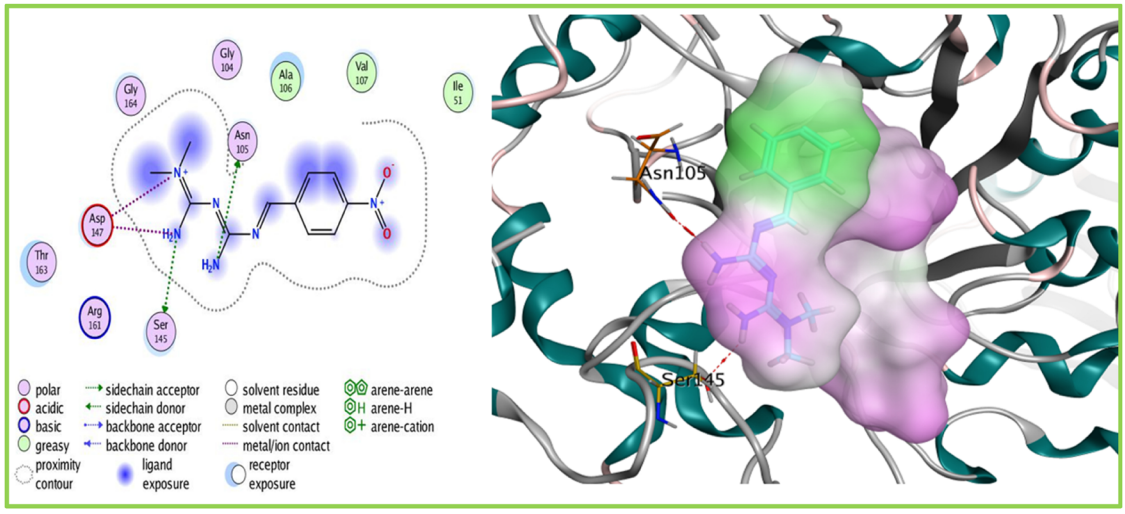

Figure 10: 2D and 3D of HL**2** at the active site of α-amylase (PDB: 1B2Y).

3.2.2 SwissADME

According to the SwissADME program's predictions, the novel metformin derivatives can be taken orally after being tested in clinical settings for their antidiabetic and antioxidant abilities, where a high level of antidiabetic and antioxidant activity is shown by the *in vitro* findings.

The five criteria laid out by Lipinski, upon which the SwissADME program is based are MWs in the range (150–500) g/mol, hydrogen bond acceptors (HBA) must be less than 10, hydrogen bond donors (HBD) should be less than 5, TPSA which is between 20 and 130 $Å^2$, and lastly, high LIPO needed of XLOGP3 g(LogP < 5). In contrast, the proposed compounds are considered unsuitable for drug-likeness if they violate more than two of Lipinski's five rules. Table 7 displays ADME predictions for HL**1** and HL**2**, as well as metformin and ascorbic acid, and demonstrates that HL**1** and HL**2**, which adhered to Lipinski's five criteria, also possess the chemical and physical qualities necessary for oral bioavailability [62].

HL1 and HL2 have molecular weights of 262.27 g/mol, which are within the permitted limit; the number of rotatable bonds of the derivatives of metformin is equal to 6, indicating good structural flexibility; there are 5 (HBA) and 3 (HBD), both acceptors and donors falling inside the required range, TPSA has gained increased importance in medicinal chemistry. When the TPSA value is greater than 60 $Å^2$ and less than 130 $Å^2$, it can be used to accurately predict intestinal absorption; when it is less than 60 $Å^2$, it shows excellent blood–brain barrier permeability. Metformin derivatives have TPSA values of 121.15 $Å^2$, which means they will be more readily absorbed in the gastrointestinal tract, which has a 68.48% absorption rate, but the absorbance of the standard drugs is higher. In order for a new synthetic molecule to meet Lipinski's rules, it must have adequate oral and intestinal absorption, which is necessary for it to be drug-like, and the value of Log p must be less than 5. The values of XLOGP3 for the Schiff bases fall within the ideal range for LIPO and the examined HL**1** and HL**2** have drug-like properties that can be easily determined using bioavailability radars; these parameters are indicated by the pink region through the ideal range for each feature (LIPO, size, solubility, polarity, flexibility, and saturation) as well as standard drugs as displayed in Figures 12–15. Moreover, the range of synthetic accessibility was 2.80 to 3.04; consequently, there is a good chance of synthesizing all of them.

Oral medication must be able to penetrate either the intestinal or brain barrier; thus, both of them are the most crucial ADMET features, assigned by BBB and GI in Table 7,

Table 6: Docking results of HL**1**, HL**2**, and metformin with 1B2Y

Ligand	Ligand–protein interactions	Type of bond/ bond length (Å)	Docking score (kcal/mol)
HL**1**	Lig-NH-H—O-SER145	H-donor/3.17	−5.41
	Lig-NH-H—O-ASN105	H-donor/3.36	
	Lig-NH-H—O-ASP147	H-donor/2.85	
	Lig-N—O-ASP147	Ionic/3.34	
HL**2**	Lig-NH-H—O-SER145	H-donor/3.33	−5.47
	Lig-NH-H—O-ASN105	H-donor/3.05	
	Lig-N—O-ASP147	Ionic/3.33	
	Lig-N—O-ASP147	Ionic/3.90	
Metformin	Lig-NH-H—O-LEU162	H-donor/3.28	−4.95

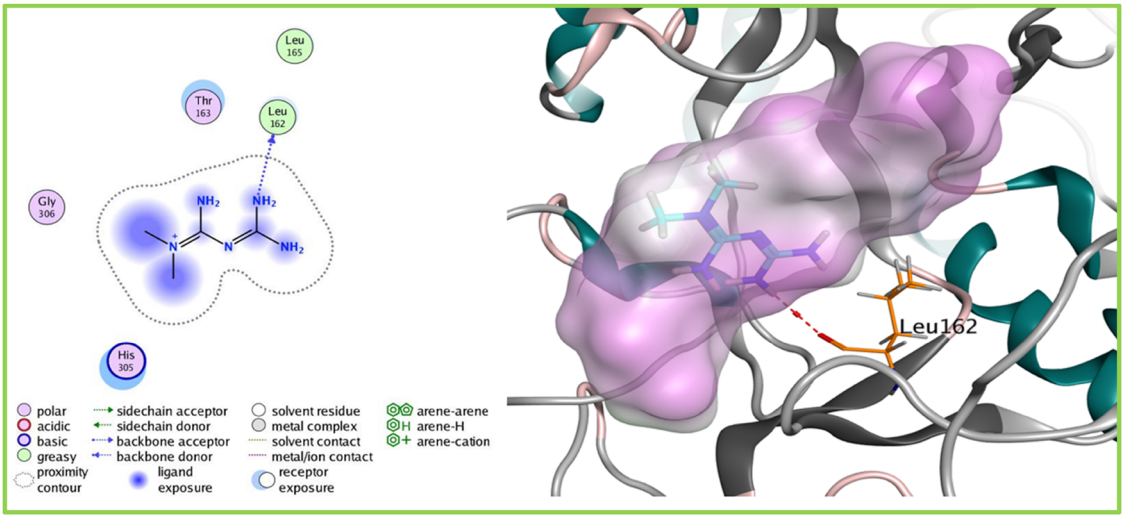

Figure 11: 2D and 3D of metformin at the active site of α-amylase (PDB: 1B2Y).

Table 7: SwissADME predictions for HL1, HL2, metformin, and ascorbic acid

Properties	HL1	HL2	Metformin	Ascorbic acid	
Physicochemical	MW (<500 Da)	262.27 g/mol	262.27 g/mol	165.62 g/mol	176.12 g/mol
	RP < 9	6	6	3	2
	HBA (<10)	5	5	2	6
	HBD (<5)	3	3	4	4
	TPSA	121.15 Å^2	121.15 Å^2	88.99 Å^2	107.22 Å^2
	ABS%	68.48	68.48	79.23	73.13
	Fraction Csp3	0.18	0.18	0.50	0.50
Pharmacokinetics	XLOGP3 (LogP < 5)	1.07	1.07	−0.26	−1.64
	GIA	High	High	High	High
	BBBP	No	No	No	No
	PgPS	No	No	No	No
	CYP1A2 inhibition	No	No	No	No
	CYP2C19 inhibition	No	No	No	No
	CYP2C9 inhibition	No	No	No	No
	CYP2D6 inhibition	No	No	No	No
	CYP3A4 inhibition	No	No	No	No
	Log Kp (cm/s)	−7.14 cm/s	−7.14 cm/s	−7.49 cm/s	−8.54 cm/s
Druglikeness	LV	0	0	0	0
	BS	0.55	0.55	0.55	0.56
Medicinal chemistry	LLV	Yes	Yes	1	1
	SA	3.04	2.80	3.11	3.47

MW: molecular weight, RP: number of rotatable bonds, HBA: number of hydrogen bond acceptors (O and N atoms), HBD: number of hydrogen bond donors (OH and NH groups), TPSA: molecular polar surface area, %ABS = 109 − (0.3345 × TPSA), Csp3: the fraction of carbon bond saturation (Csp3), XLOGP3 (LogP < 5): lipophilicity parameter, GIA = gastrointestinal absorption, BBBP = blood–brain barrier permeation, PgPS = P-glycoprotein substrate, Log Kp: skin permeability parameter, CYP1A2, CYP3A4, CYP2C9, CYP2C19, and CYP2D6: the five main cytochrome p450 (CYP) enzyme isoforms, which biotransform more than 50–90% of pharmaceutical compounds, LV: number of "Rule of five" violations, BS: bioavailability score, LLV: lead likeness violations, SA: synthetic accessibility.

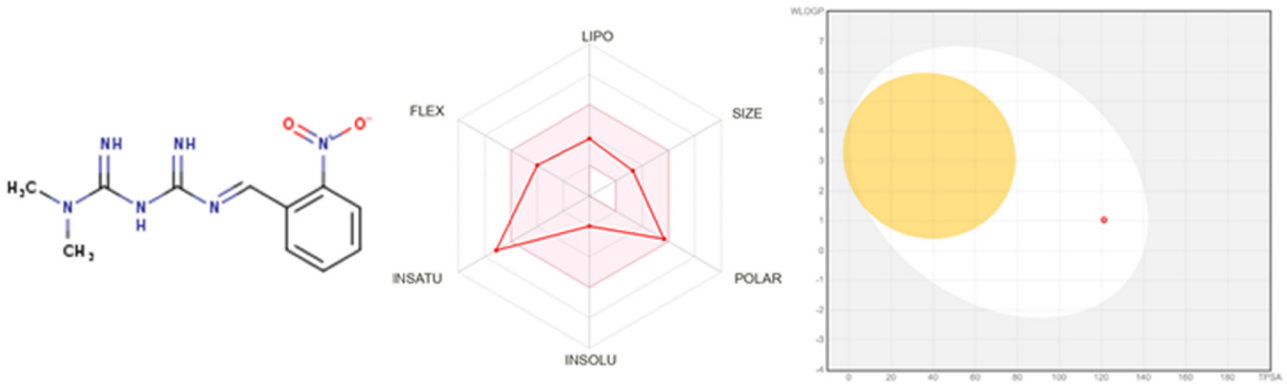

Figure 12: Structure, bioavailability radar, and the Boiled-Egg graph of HL1 based on SwissADME.

and illustrated by the BOILED-Egg. According to the ADME prediction, molecules in the white region have a higher chance of being absorbed by the GI tract, but those in the yellow zone are more likely to penetrate the brain. Metformin derivatives were not expected to permeate the brain and had a high intestinal absorption rate, as evidenced by their placement inside the white region in Figures 12 and 13, and the basic function of P-glycoprotein (P-gp) is to protect the body from toxic substances by maintaining the BBB and removing medications from the kidneys and liver into urine and bile, since metformin derivatives have no effect on the permeability of gp, in addition, the data in Table 7 reveal that the metformin derivative has no effect on the excretion or functionality

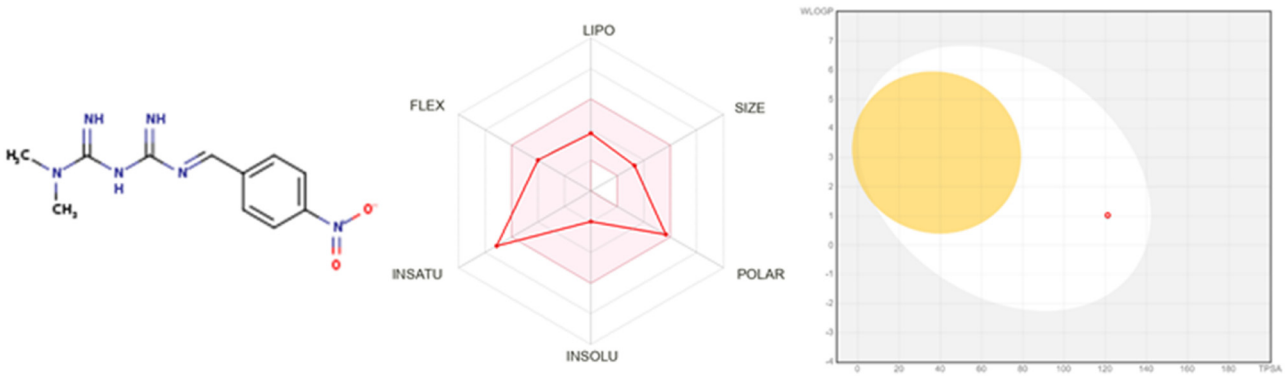

Figure 13: Structure, bioavailability radar, and the Boiled-Egg graph of HL2 based on SwissADME.

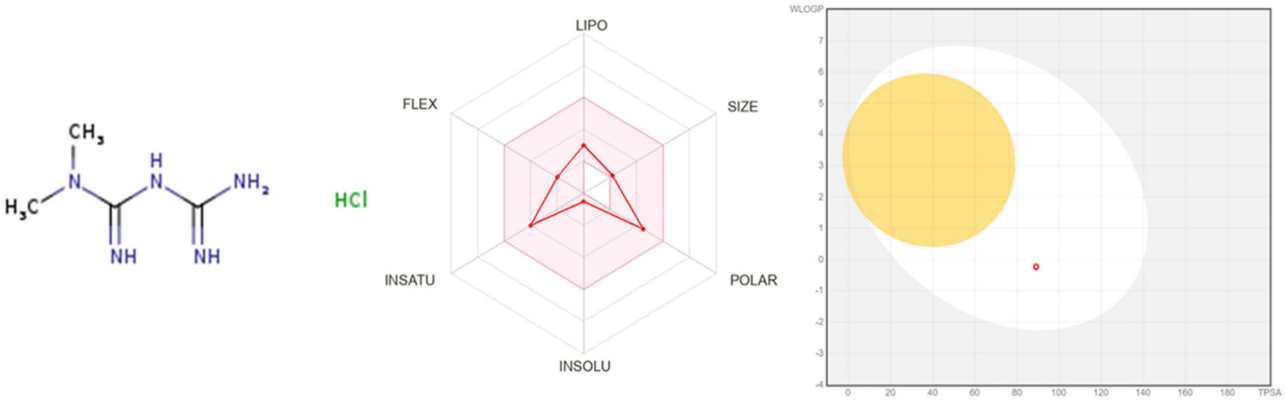

Figure 14: Structure, bioavailability radar, and the Boiled-Egg graph of metformin based on SwissADME.

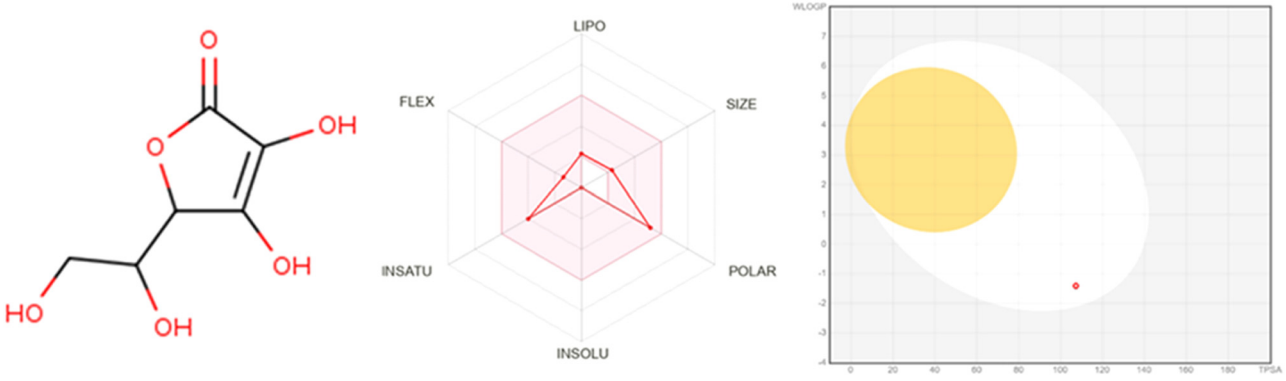

Figure 15: Structure, bioavailability radar, and the Boiled-Egg graph of ascorbic acid based on SwissADME.

of the five CYP enzymes confirming that the new drug will be properly metabolized and will not accumulate. Also, derivatives of metformin showed skin permeability values of −7.14 cm/s, which are within the acceptable range of Log Kp for drug candidates [56,57,63].

4 Conclusions

Experiments done *in vitro* on the alpha-amylase enzyme, the sucrase enzyme, and the DPPH scavenging radical for antidiabetic and antioxidant purposes showed excellent

results that were in line with theoretical studies. HL**2** displayed superior inhibitory activity on the alpha-amylase enzyme, while HL**1** showed a more powerful effect on the sucrase enzyme. By contrast, the DPPH assay revealed that maximum antioxidant activity was shown by HL2, followed by ascorbic acid and HL**1**, using the DPPH assay. The A549 lung cancer cell line was the subject of our investigation, which demonstrated that both HL1 and HL2 have anticancer potential. However, HL1 had superior activity. The anticancer effect against other cancer cell lines will need to be investigated further, though. Furthermore, the molecular docking study demonstrated that HL**1** and HL**2** interacted strongly at the active sites of the targeted proteins 2CDU and 1B2Y, with HL**2** being the most potent α-amylase enzyme inhibitor and the best antioxidant. In contrast, the ADME predictions of metformin derivatives suggest that these compounds have good bioavailability and adhere to Lipinski's five principles. As was previously stated and is evident from all outcomes, metformin derivatives are a strong option for therapeutic usage, but additional studies are required to support these findings, first on rats and then subsequently on human patients.

Acknowledgments: The authors extend their appreciation to the Researchers Supporting Project number (RSPD2023R755), King Saud University, Riyadh, Saudi Arabia.

Funding information: The work was financially supported by Researchers Supporting Project number (RSPD2023R755), King Saud University, Riyadh, Saudi Arabia.

Author contributions: Abdel-Basit Al-Odayni – conceptualization; Waseem Sharaf Saeed and Ahmad Al-Owais – data curation; Inas Al-Qadsy, Lena Al-Faqeeh, and Abdelhabib Semlali – formal analysis; Waseem Sharaf Saeed – funding acquisition; Inas Al-Qadsy and Ali Alrabie – investigation; Inas Al-Qadsy and Lena Al-Faqeeh – methodology; Mazahar Farooqui – project administration; Abdel-Basit Al-Odayni and Ahmad Al-Owais – resources; Inas Al-Qadsy and Ali Alrabie – software; Mazahar Farooqui – upervision; Abdelhabib Semlali – validation; Waseem Sharaf Saeed, Arwa Al-Adhreai and Mazahar Farooqui – visualization; Inas Al-Qadsy – writing – original draft; Inas Al-Qadsy, Waseem Sharaf Saeed, Abdelhabib Semlali and Mazahar Farooqui – writing – review & editing.

Conflict of interest: The authors declare no conflict of interest.

Ethical approval: The conducted research is not related to either human or animal use.

Data availability statement: All data generated or analyzed during this study are included in this published article.

References

[1] Morsy NM, Hassan AS, Hafez TS, Mahran MR, Sadawe IA, Gbaj AM. Synthesis, antitumor activity, enzyme assay, DNA binding and molecular docking of Bis-Schiff bases of pyrazoles. J Iran Chem Soc. 2021;18:47–59.

[2] Mukhtar SS, Hassan AS, Morsy NM, Hafez TS, Hassaneen HM, Saleh FM. Overview on synthesis, reactions, applications, and biological activities of Schiff bases. Egypt J Chem. 2021;64(11):6541–54.

[3] Omidi S, Kakanejadifard A. A review on biological activities of Schiff base, hydrazone, and oxime derivatives of curcumin. RSC Adv. 2020;10(50):30186–202.

[4] Yakan H, Omer H-H, Buruk O, Çakmak Ş, Marah S, Veyisoğlu A, et al. Synthesis, structure elucidation, biological activity, enzyme inhibition and molecular docking studies of new Schiff bases based on 5-nitroisatin-thiocarbohydrazone. J Mol Structure. 2023;1277:134799.

[5] Kansız S, Dege N, editors. Characterization and structural investigations of Schiff based pentafluorinated derivative compound. International Conference on Frontiers in Academic Research; 2023.

[6] Al-Qadsy I, Saeed WS, Al-Odayni A-B, Ahmed Saleh Al-Faqeeh L, Alghamdi AA, Farooqui M. Novel metformin-based Schiff bases: synthesis, characterization, and antibacterial evaluation. Materials. 2020;13(3):514.

[7] Association AD. Diagnosis and classification of diabetes mellitus. Diabetes care. 2005;28(1):S37.

[8] Fröde T, Medeiros Y. Animal models to test drugs with potential antidiabetic activity. J Ethnopharmacol. 2008;115(2):173–83.

[9] Al-Faqeeh LAS, Naser R, Kagne S, Khan SW. Activity of mushrooms against diabetic and inflammation: A review. GSC Biol Pharm Sci. 2021;14(2):37–44.

[10] Keerthana G, Kalaivani M, Sumathy A. In-vitro alpha amylase inhibitory and anti-oxidant activities of ethanolic leaf extract of Croton bonplandianum. Asian J Pharm Clin Res. 2013;6(4):32–6.

[11] Li W, Zheng H, Bukuru J, De, Kimpe N. Natural medicines used in the traditional Chinese medical system for therapy of diabetes mellitus. J Ethnopharmacol. 2004;92(1):1–21.

[12] Ravi B, Renitta RE, Prabha ML, Issac R, Naidu S. Evaluation of antidiabetic potential of oyster mushroom (Pleurotus ostreatus) in alloxan-induced diabetic mice. Immunopharmacol Immunotoxicol. 2013;35(1):101–9.

[13] Tasyurek HM, Altunbas HA, Balci MK, Sanlioglu S. Incretins: their physiology and application in the treatment of diabetes mellitus. Diabetes/Metab Res Rev. 2014;30(5):354–71.

[14] Warraich HJ, Rana JS. Diabetic dyslipidemia: epidemiology and prevention of cardiovascular disease and implications of newer therapies. Curr Cardiol Rep. 2018;20:1–7.

[15] Mishra SB, Vijayakumjar M, Ojha SK, Verma A. Antidiabetic effect of Jatropha curcas L. leaves extract in normal and alloxan-induced diabetic rats. Int J Ph Sci. 2010;2(1):482–7.

[16] Milani E, Nikfar S, Khorasani R, Zamani MJ, Abdollahi M. Reduction of diabetes-induced oxidative stress by phosphodiesterase inhibitors in rats. Comp Biochem Physiol Part C: Toxicol & Pharmacology. 2005;140(2):251–5.

[17] Khan RMM, Chua ZJY, Tan JC, Yang Y, Liao Z, Zhao Y. From pre-diabetes to diabetes: diagnosis, treatments and translational research. Medicina. 2019;55(9):546.
[18] Singh SK, Rai PK, Jaiswal D, Watal G. Evidence-based critical evaluation of glycemic potential of Cynodon dactylon. Evidence-Based Complementary Alternative Med. 2008;5:415–20.
[19] Malviya N, Jain S, Malviya S. Antidiabetic potential of medicinal plants. Acta Pol Pharm. 2010;67(2):113–8.
[20] Etxeberria U, de la Garza AL, Campión J, Martínez JA, Milagro FI. Antidiabetic effects of natural plant extracts via inhibition of carbohydrate hydrolysis enzymes with emphasis on pancreatic alpha amylase. Expert Opin Ther Targets. 2012;16(3):269–97.
[21] Eddouks M, Maghrani M, Lemhadri A, Ouahidi M-L, Jouad H. Ethnopharmacological survey of medicinal plants used for the treatment of diabetes mellitus, hypertension and cardiac diseases in the south-east region of Morocco (Tafilalet). J Ethnopharmacol. 2002;82(2–3):97–103.
[22] Shukia R, Sharma S, Puri D, Prabhu K, Murthy P. Medicinal plants for treatment of diabetes mellitus. Indian J Clin Biochem. 2000;15:169–77.
[23] Chang CH, Lin JW, Wu LC, Lai MS, Chuang LM, Arnold Chan K. Association of thiazolidinediones with liver cancer and colorectal cancer in type 2 diabetes mellitus. Hepatology. 2012;55(5):1462–72.
[24] Hassan AS, Morsy NM, Aboulthana WM, Ragab A. Exploring novel derivatives of isatin-based Schiff bases as multi-target agents: design, synthesis, *in vitro* biological evaluation, and in silico ADMET analysis with molecular modeling simulations. RSC Adv. 2023;13(14):9281–303.
[25] Dujic T, Causevic A, Bego T, Malenica M, Velija-Asimi Z, Pearson E, et al. Organic cation transporter 1 variants and gastrointestinal side effects of metformin in patients with Type 2 diabetes. Diabet Med. 2016;33(4):511–4.
[26] Bouchoucha M, Uzzan B, Cohen R. Metformin and digestive disorders. Diabetes & Metab. 2011;37(2):90–6.
[27] Al-Faqeeh LAS, Naser R, Kagne S, Khan SW. Nutritional values, ethno-medicinal uses and antioxidant activity of mushrooms: A review. Eur J Biomed. 2021;8:292–300.
[28] Lushchak VI. Free radicals, reactive oxygen species, oxidative stress and its classification. Chemico-Biological Interact. 2014;224:164–75.
[29] Ferreira IC, Barros L, Abreu R. Antioxidants in wild mushrooms. Curr Medicinal Chem. 2009;16(12):1543–60.
[30] Phaniendra A, Jestadi DB, Periyasamy L. Free radicals: properties, sources, targets, and their implication in various diseases. Indian J Clin Biochem. 2015;30:11–26.
[31] Qazi MA, Molvi KI. Free radicals and their management. Am J Pharm Health Res. 2018;6(4):1–10.
[32] Blokhina O, Virolainen E, Fagerstedt KV. Antioxidants, oxidative damage and oxygen deprivation stress: a review. Ann botany. 2003;91(2):179–94.
[33] Ridnour LA, Thomas DD, Mancardi D, Espey MG, Miranda KM, Paolocci N, et al. The chemistry of nitrosative stress induced by nitric oxide and reactive nitrogen oxide species. Putting Perspective on Stressful Biological Situations; 2004.
[34] Kozarski M, Klaus A, Jakovljevic D, Todorovic N, Vunduk J, Petrović P, et al. Antioxidants of edible mushrooms. Molecules. 2015;20(10):19489–525.
[35] Rai M, Biswas G, Mandal S, Acharya K. Free radicals and human diseases. Herbal drugs: A modern approach to understand them better. India: New Central Book Agency; 2011.
[36] Valko M, Leibfritz D, Moncol J, Cronin MT, Mazur M, Telser J. Free radicals and antioxidants in normal physiological functions and human disease. Int J Biochem Cell Biol. 2007;39(1):44–84.
[37] Halliwell B. Biochemistry of oxidative stress. Biochem Soc Trans. 2007;35(5):1147–50.
[38] Demir S, Cakmak S, Dege N, Kutuk H, Odabasoglu M, Kepekci RA. A novel 3-acetoxy-2-methyl-*N*-(4-methoxyphenyl) benzamide: Molecular structural describe, antioxidant activity with use X-ray diffractions and DFT calculations. J Mol Structure. 2015;1100:582–91.
[39] Wang Y-W, He S-J, Feng X, Cheng J, Luo Y-T, Tian L, et al. Metformin: a review of its potential indications. Drug Design, Dev Ther. 2017;2421–9.
[40] Shurrab NT, Arafa E-SA. Metformin: A review of its therapeutic efficacy and adverse effects. Obes Meicine. 2020;17:100186.
[41] Gronich N, Rennert G. Beyond aspirin – cancer prevention with statins, metformin and bisphosphonates. Nat Rev Clin Oncol. 2013;10(11):625–42.
[42] Samuel VP, Dahiya R, Singh Y, Gupta G, Sah SK, Gubbiyappa SK, et al. Metformin: a salutary candidate for colorectal cancer treatment in patients with diabetes. J Environ Pathology, Toxicol Oncol. 2019;38(2):133–41.
[43] Yu H, Zhong X, Gao P, Shi J, Wu Z, Guo Z, et al. The potential effect of metformin on cancer: an umbrella review. Front Endocrinol. 2019;10:617.
[44] Puneeth HR, Sharada AC. Antidiabetic effects of a series of curcumin pyrazoles in-vitro. Asian J Pharm. Clin Res. 2015;8(6):146–9.
[45] Sharath Chandra SPSK, Puneeth HR, Sharada AC. Comparative evaluation of 6-fluoro-3-(piperidin-4-yl) benzo[d] isoxazole derivatives and atypical antipsychotics for their anti-diabetic properties. Int J Bioassays. 2015;4(06):3964–7.
[46] Nasr FA, Shahat AA, Alqahtani AS, Ahmed MZ, Qamar W, Al-Mishari AA, et al. Centaurea bruguierana inhibits cell proliferation, causes cell cycle arrest, and induces apoptosis in human MCF-7 breast carcinoma cells. Mol Biol Rep. 2020;47:6043–51.
[47] Edziri H, Mastouri M, Mahjoub MA, Mighri Z, Mahjoub A, Verschaeve L. Antibacterial, antifungal and cytotoxic activities of two flavonoids from Retama raetam flowers. Molecules. 2012;17(6):7284–93.
[48] Sherif AY, Harisa GI, Shahba AA, Alanazi FK, Qamar W. Optimization of gefitinib-loaded nanostructured lipid carrier as a biomedical tool in the treatment of metastatic lung cancer. Molecules. 2023;28(1):448.
[49] Costa JD, Ramos RD, Costa KD, Brasil DD, Silva CH, Ferreira EF, et al. An in silico study of the antioxidant ability for two caffeine analogs using molecular docking and quantum chemical methods. Molecules. 2018;23(11):2801.
[50] Settu R, Selvaraj D, Padikasan IA. GCMS profiling and in silico screening of alpha-amylase inhibitors in traditional pigmented rice varieties (Oryza sativa Linn) of Tamil Nadu. Food Biosci. 2021;42:101154.
[51] Majumdar M, Singh V, Misra TK, Roy DN. In silico studies on structural inhibition of SARS-CoV-2 main protease Mpro by major secondary metabolites of Andrographis paniculata and Cinchona officinalis. Biologia. 2022;77(5):1373–89.
[52] Alrabie A, Al-Dhreai A, Al-Qadsy I, Pradhan V, Farooqui M. Phytochemical Screening, GC-MS analysis, Molecular docking study and evaluation of antioxidant and antimicrobial activity of Sapindus emarginatus seed kernel. RJPT. 2022;15(5):2117–21.

[53] Tamer Ö, Mahmoody H, Feyzioğlu KF, Kılınç O, Avci D, Orun O, et al. Synthesis of the first mixed ligand Mn (II) and Cd (II) complexes of 4-methoxy-pyridine-2-carboxylic acid, molecular docking studies and investigation of their anti-tumor effects *in vitro*. Appl Organomet Chem. 2020;34(3):e5416.
[54] Alrabie A, Al-Rabie NA, Al Saeedy M, Al Adhreai A, Al-Qadsy I, Farooqui M. Martynia annua safety and efficacy: heavy metal profile, in silico and *in vitro* approaches on antibacterial and anti-diabetic activities. Nat Product Res. 2022;1–7.
[55] Kansız S, Tolan A, Azam M, Dege N, Alam M, Sert Y, et al. Acesulfame based Co (II) complex: Synthesis, structural investigations, solvatochromism, Hirshfeld surface analysis and molecular docking studies. Polyhedron. 2022;218:115762.
[56] Ranjith D, Ravikumar C. SwissADME predictions of pharmacokinetics and drug-likeness properties of small molecules present in Ipomoea mauritiana Jacq. J Pharmacognosy Phytochemistry. 2019;8(5):2063–73.
[57] Sravika N, Priya S, Divya N, Jyotsna PMS, Anusha P, Kudumula N, et al. Swiss ADME properties screening of the phytochemical compounds present in Bauhinia acuminata. J Pharmacogn Phytochem. 2021;10(4):411–9.
[58] Sreejayan N, Rao M. Free radical scavenging activity of curcuminoids. Arzneimittel-forschung. 1996;46(2):169–71.
[59] Sánchez-Moreno C. Methods used to evaluate the free radical scavenging activity in foods and biological systems. Food Sci Technol Int. 2002;8(3):121–37.
[60] Alqahtani AS, Ghorab MM, Nasr FA, Ahmed MZ, Al-Mishari AA, Attia SM. The antiproliferative and apoptotic effects of a novel quinazoline carrying substituted-sulfonamides: *in vitro* and molecular docking study. Molecules. 2022;27(3):981.
[61] Hanif A, Ibrahim AH, Ismail S, Al-Rawi SS, Ahmad JN, Hameed M, et al. Cytotoxicity against A549 human lung cancer cell line via the mitochondrial membrane potential and nuclear condensation effects of nepeta paulsenii briq., a perennial herb. Molecules. 2023;28(6):2812.
[62] Arwa A-A, ALSaeedy M, Alrabie A, Al-Qadsy I, Dawbaa S, Alaizeri ZM, et al. Design and synthesis of novel enantiopure Bis (5-Isoxazolidine) derivatives: insights into their antioxidant and antimicrobial potential via in silico drug-likeness, pharmacokinetic, medicinal chemistry properties, and molecular docking studies. Heliyon. 2022;8(6):e09746.
[63] Daina A, Michielin O, Zoete V. SwissADME: A free web tool to evaluate pharmacokinetics, drug-likeness and medicinal chemistry friendliness of small molecules. Sci Rep. 2017;7(1):42717.